Free Radical Biology and Medicine 150 (2020) 148–160

Contents lists available at ScienceDirect

Free Radical Biology and Medicine

journal homepage: www.elsevier.com/locate/freeradbiomed

# 17β-estradiol ameliorates lipotoxicity-induced hepatic mitochondrial oxidative stress and insulin resistance

Bel M. Galmés-Pascual[a,b], Melanie Raquel Martínez-Cignoni[a,b], Andrea Morán-Costoya[a], Marco Bauza-Thorbrügge[a,b,1], Miquel Sbert-Roig[a,b], Adamo Valle[a,b,c,*], Ana M. Proenza[a,b,c], Isabel Lladó[a,b,c], Magdalena Gianotti[a,b,c]

[a] Grup Metabolisme Energètic i Nutrició, Departament de Biologia Fonamental i Ciències de la Salut, Institut Universitari d'Investigació en Ciències de la Salut (IUNICS), Universitat de les Illes Balears, Ctra. Valldemossa, km 7.5, E-07122, Palma de Mallorca, Illes Balears, Spain
[b] Institut d'Investigació Sanitària Illes Balears (IdISBa), Hospital Universitari Son Espases, E-07120, Palma de Mallorca, Illes Balears, Spain
[c] Centro de Investigación Biomédica en Red Fisiopatología de la Obesidad y Nutrición (CIBERobn, CB06/03/0043), Instituto de Salud Carlos III, E- 28029, Madrid, Spain

ARTICLE INFO

*Keywords:*
Sex dimorphism
Liver steatosis
ROS
JNK
Mitochondrial function
Insulin resistance

ABSTRACT

The prevalence and severity of nonalcoholic fatty liver disease (NAFLD) is higher in men and postmenopausal women compared to premenopausal women, suggesting a protective role for ovarian hormones. Diet-induced obesity and fatty acids surplus promote mitochondrial dysfunction in liver, triggering oxidative stress and activation of c-Jun N-terminal kinase (JNK) which has been related to the development of insulin resistance and steatosis, the main hallmarks of NAFLD. Considering that estrogen, in particular 17β-estradiol (E2), have been reported to improve mitochondrial biogenesis and function in liver, our aim was to elucidate the role of E2 in preventing fatty acid-induced insulin resistance in hepatocytes through modulation of mitochondrial function, oxidative stress and JNK activation. An *in vivo* study was conducted in Wistar rats of both sexes ($n = 7$) fed control diet and high-fat diet (HFD), and in vitro studies were carried out in HepG2 cells treated with palmitate (PA) and E2 for 24 h. Our HFD-fed male rats showed a prediabetic state characterized by greater systemic and hepatic insulin resistance, as well as higher lipid content in liver, compared to females. JNK activation rose markedly in males in response to HFD feeding, in parallel with mitochondrial dysfunction and oxidative stress. Consistently, in PA-exposed HepG2 cells, E2 treatment prevented JNK activation, insulin resistance and fatty acid accumulation. Altogether, our data highlights the importance of E2 as a mitigating factor of fatty acid-insulin resistance in hepatocytes through downregulation of JNK activation, by means of mitochondrial function improvement.

## 1. Introduction

Hypercaloric diet and sedentary lifestyle are major causes of metabolic syndrome, which is characterized by the combination of disorders including obesity, dyslipidaemia, insulin resistance, diabetes, and cardiovascular disease, among others [1]. Nonalcoholic fatty liver disease (NAFLD) is defined as excessive fat accumulation within the liver, in the absence of significant alcohol consumption or any secondary cause, and is increasingly recognized as the hepatic manifestation of metabolic syndrome [1]. High fat diets (HFD) and obesity are associated with increased free fatty acids (FFA) flux into the bloodstream thereby leading to enhanced fatty acid uptake in liver [2]. Hepatic fat accumulation arises from an imbalance between lipid storage (fatty acid uptake and de novo lipogenesis) and lipid removal (fatty acid oxidation and export as a component of VLDL particles) [3]. Free fatty acid surplus and lipid species such as ceramides or DAG accumulation in liver contribute to the development and exacerbation of hepatic insulin resistance [4,5].

In postmenopausal women and ovariectomized (OVX) animal models, loss of estrogens is linked to an increase in central adiposity, insulin resistance and the development of complications such as hepatic steatosis and type 2 diabetes [6]. Estrogen protection is suggested in human studies, where the prevalence of NAFLD is lower in premenopausal women compared to men or postmenopausal women

* Corresponding author. Universitat de les Illes Balears, Ctra. Valldemossa, km 7.5, E-07122, Palma de Mallorca, Illes Balears, Spain.
*E-mail address:* adamo.valle@uib.es (A. Valle).
[1] Department of Physiology/Metabolic Physiology, Institute of Neuroscience and Physiology, The Sahlgrenska Academy at University of Gothenburg, Box 432, SE-405 30, Gothenburg, Sweeden

https://doi.org/10.1016/j.freeradbiomed.2020.02.016
Received 13 November 2019; Received in revised form 11 February 2020; Accepted 19 February 2020
Available online 24 February 2020

**Abbreviations**

| | |
|---|---|
| NAFLD | nonalcolholic fatty liver disease |
| HFD | high fat diet |
| FFA | free fatty acids |
| OVX | ovariectomized |
| ROS | reactive oxygen species |
| E2 | 17β-estradiol |
| JNK | c-Jun N-terminal kinase |
| IRS | insulin receptor substrate |
| PA | palmitate |
| TG | triglyceride |
| PEPCK | phosphoenolpyruvate carboxykinase |
| PPARα/PPARγ | peroxisome proliferator activated receptor α/γ |
| SREBP-1c | sterol regulatory element binding transcription factor 1c |
| PGC-1α/PGC-1β | peroxisome proliferator-activated receptor gamma coactivator 1α/1β |
| TFAM | mitochondrial transcription factor A |
| UCP2 | uncoupling protein 2 |
| mtDNA | mitochondrial DNA |
| TAC | total non-enzymatic antioxidant capacity |
| MnSOD | manganese superoxide dismutase |
| MMP | mitochondrial membrane potential |
| FBS | fetal bovine serum |

[7–11], and insulin sensitivity remains higher in women than in men [12,13]. Accordingly, non-obese male rats show reduced systemic insulin sensitivity and a slower hepatic response to insulin, in comparison with females [14], as well as a higher degree of lipid accumulation in the liver when fed a HFD [15]. All in all, these data suggest a protective role for female sex hormones against insulin resistance and liver steatosis, although the underlying mechanisms are poorly understood.

Accumulating evidence points towards hepatic mitochondrial dysfunction playing a critical role in the development of NAFLD. Ultrastructural and functional abnormalities in mitochondria, and subsequently reactive oxygen species (ROS) formation, are associated with NAFLD [16]. Estrogens are well-known regulators of mitochondrial biogenesis and function [17]. Recently, we have reported an enhancement of mitochondrial function and biogenesis by 17β-estradiol (E2) treatment in hepatocytes [18], so it is plausible to consider a better prognosis of steatosis in females due to the protective role of E2 in mitochondrial function. The activation of c-Jun N-terminal kinase (JNK), a mitogen-activated protein kinase family member, plays a central role in the cell stress response, with outcomes ranging from cell death to cell proliferation and survival, depending on the specific context (reviewed in Ref. [19]). Sustained JNK activation in liver has been related to the development of insulin resistance and steatosis; attracting attention as a key mediator of the pathogenesis of NAFDL [20]. Diverse stimuli, including several drugs, oxidative stress and lipotoxic insults, are recognized to lead to sustained JNK activation through a feedback loop mechanism involving mitochondria and ROS [21,22]. In turn, JNK phosphorylates insulin receptor substrate (IRS) 1 at serine 307 leading to reduced Akt phosphorylation and a consequent inhibition of insulin signalling [23].

In light of the above considerations, the aim of this study was to investigate the factors involved in E2 effects in decreasing hepatic insulin resistance associated with lipotoxic conditions. To test this, we performed studies in both male and female rats fed an HFD, and HepG2 hepatocytes treated with palmitate (PA) to induce lipotoxicity, and E2 to elucidate the contribution of this hormone in processes underlying hepatic insulin resistance.

## 2. Results

### 2.1. Body weight, adiposity, glucose tolerance and lipemia in HFD-fed male and female rats

High fat/high sucrose diet (HFD) for 16 weeks increased body weight (Fig. 1A) in both sexes (11,7% in males, 15% in females). Although no sex differences were found in body weight gain, the increase in adiposity index (Fig. 1B) was significantly higher in male (97%) compared to female rats (44%). To assess the effects of diet on glycaemic control, glucose tolerance test was performed four days prior to sacrifice. As shown in Fig. 1C and D, HFD-fed male rats exhibited impaired glucose tolerance compared to females. Although fasted glucose levels were similar between sex and diet groups (data not shown), insulin levels were markedly increased in HFD-fed male rats (Fig. 1E). HOMA-IR confirmed insulin resistance in HFD-fed male rats, suggesting a prediabetic state in this sex under our HFD conditions (Fig. 1F). Accordingly, lipemia was also more altered by HFD in this sex (Fig. 1G-I), with higher circulating levels of triglycerides, cholesterol and FFA.

### 2.2. Lipid accumulation in liver of HFD-fed male and female rats and in HepG2 cells treated with PA and E2

HFD-feeding increased liver weight only in male rats (Fig. 2A). Although hepatic lipid content increased in both sexes, it was more pronounced in males. Interestingly, free fatty acids, which excessive tissular levels have been widely related to lipotoxicity, were also increased in response to HFD in male rats. To better characterize lipid metabolism in liver of these animals, expression levels of master regulators of lipid homeostasis were analysed (Fig. 2B). The lipogenic sterol regulatory element binding transcription factor 1c (SREBP-1c) mRNA levels did not change with HFD feeding, although females exhibited lower levels compared to males. Similarly, female also showed lower levels of the lipogenic peroxisome proliferator-activated receptor γ (PPARγ) in both diet conditions. In addition, this difference was accentuated by HFD feeding since this factor was upregulated specifically in males. In contrast, the master regulator of lipid oxidation, PPARα, showed no sex differences in control conditions but it was significantly upregulated in females with HFD. To test whether E2 may influence lipid accumulation in hepatocytes under a lipotoxic environment, oil red lipid staining was performed in HepG2 cells treated with E2 in media supplemented with 0.75 mM PA (Fig. 2C and D). Consistent with *in vivo* results, intracellular lipids increased in HepG2 cells exposed to PA oversupply with E2 attenuating the PA-induced fat accumulation. Cellular viability (Fig. 2E) was not affected by E2, whereas PA treatment decreased it by about 15%, similarly to previous studies [24].

### 2.3. Mitochondrial biogenesis in liver of HFD-fed male and female rats and in HepG2 cells treated with PA and E2

Mitochondria plays a pivotal role in lipid homeostasis and reactive oxygen species (ROS) production. To assess the influence of sex in the mitochondrial adaptations to HFD, we analysed the expression of master regulators of mitochondrial biogenesis and function. Control female rats showed elevated peroxisome proliferator-activated receptor gamma coactivator 1α and 1β (PGC-1α and PGC-1β) and mitochondrial transcription factor A (TFAM) compared with their male counterparts (Fig. 3A and C). HFD feeding decreased TFAM levels exclusively in males. In accordance, mitochondrial DNA (mtDNA) levels decreased in males by 37% whereas in females just decreased 15% in response to HFD (Fig. 3A).

Similar to our animal model, in vitro experiment with HepG2 cells treated with E2 exhibited higher levels of PGC-1β and TFAM, although PGC-1α levels were not affected by E2 (Fig. 3B and D). PA exposure increased both PGC-1α and PGC-1β, but only the last one showed an

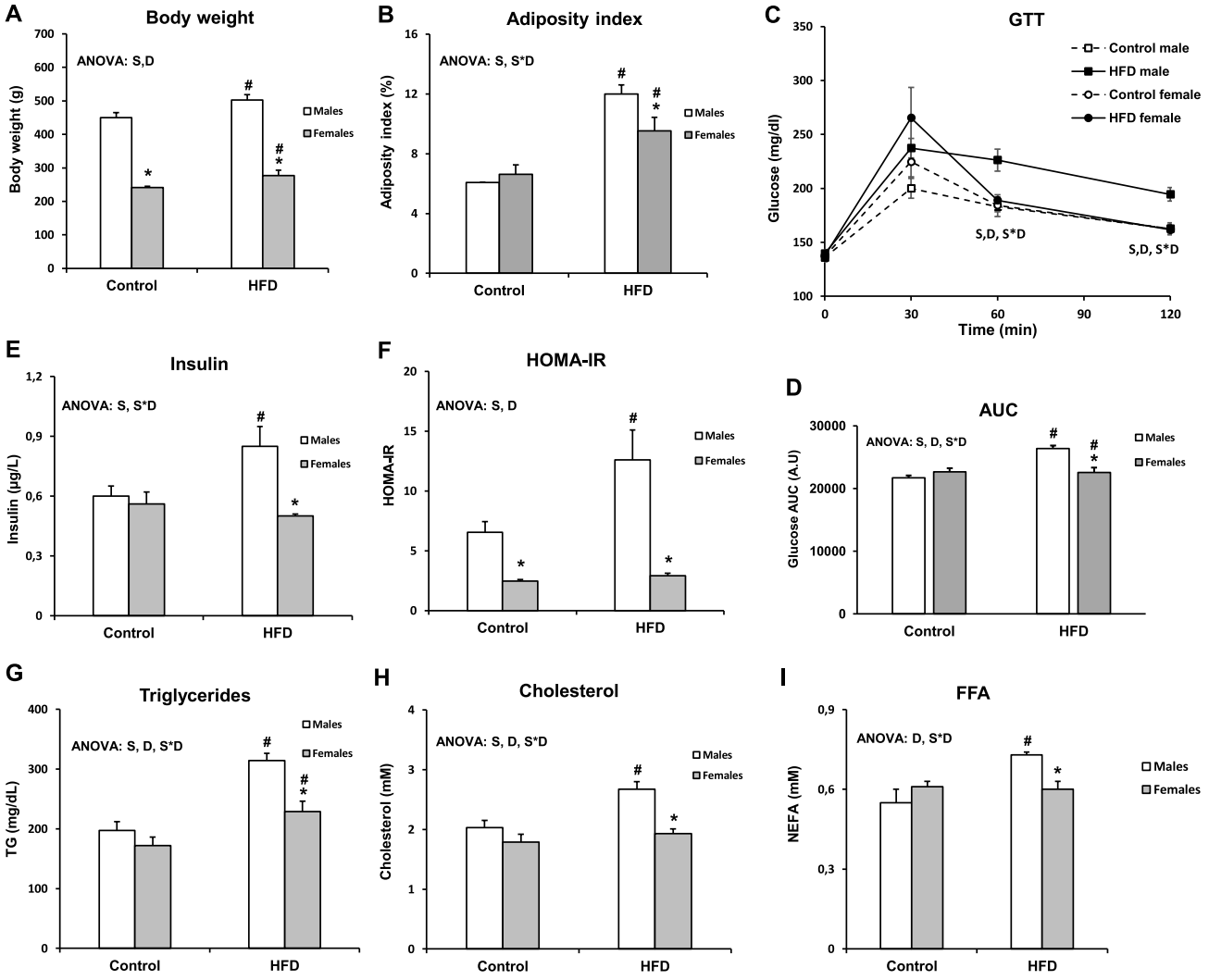


**Fig. 1.** Body weight gain, glucose tolerance test and serum parameters in HFD-fed male and female rats. A) Body weight. B) Adiposity index. C) Glucose tolerance test. Rats were fasted for a 12 h period and then plasma glucose was measured before and 15, 30, 60 and 120 min after an intraperitoneal injection of glucose (2 g/kg body weight). D) Area under the curve from glucose tolerance test. E) Serum levels of insulin. F) HOMA-IR. Serum levels of triglyceride (F), total cholesterol (G) and FFA (H). HFD, high fat diet. Values are expressed as the mean ± SEM of 7 animals per group. ANOVA ($P < 0.05$): S, sex effect; D, diet effect; S*D, sex and diet interactive effect. Student's t-test ($P < 0.05$): * male vs. female; # HFD vs. control.

enhanced expression by E2. In accordance, E2 increased mtDNA copy number in basal conditions and was able to attenuate the drop in mtDNA levels under lipotoxic conditions (Fig. 3B). From a functional point of view, the improved mitochondrial biogenesis induced by E2 translated to a higher mitochondrial membrane potential (MMP) and ATP content, consistent with the TFAM expression profile. MMP and ATP levels decreased under exposure to PA but were partially restored by E2 (Fig. 3E).

### 2.4. Oxidative stress and antioxidant capacity in liver of HFD-fed male and female rats and in HepG2 cells treated with PA and E2

To evaluate oxidative stress in liver of HFD fed rats, HNE-protein adducts, end markers of lipid peroxidation, were determined by western blot. As shown in Fig. 4A, female rats showed lower HNE levels, suggesting a higher protection against oxidative stress in both diet conditions. Lipid peroxide levels increased in liver of male rats with HFD feeding whereas in females HNE levels were equal to those under control diet. In agreement, male rats decreased their total non-enzymatic antioxidant capacity (TAC) in response to HFD, while females increased it. In addition, female rats showed higher levels of the mitochondrial antioxidant uncoupling protein 2 (UCP2) both in control and HFD conditions. In HepG2 cells, E2 showed a protective activity increasing the levels of the mitochondrial antioxidant enzyme MnSOD, and rescued catalase levels after PA exposure. Finally, ROS production in HepG2 under our experimental setting was analysed by DCFH oxidation. As shown in Fig. 4D, PA exposure induced an increase in ROS levels which was reversed by E2 treatment.

### 2.5. JNK activation and insulin resistance in liver of HFD-fed male and female rats and in HepG2 cells treated with PA and E2

ROS-induced insulin resistance is mediated by various signalling pathways, including the JNK pathway. As expected from the sex differences observed in oxidative stress, JNK activation was higher in control male rats compared to their female counterparts (Fig. 5A). HFD feeding induced JNK phosphorylation in both sexes, being this activation, once again, more pronounced in males. In accordance, E2 attenuated both basal and PA-induced JNK phosphorylation in HepG2 cells (Fig. 5B).

In relation to insulin resistance, HFD feeding reduced insulin-stimulated serine phosphorylation of Akt in male rats (Fig. 5C), whereas

that of females remained unaltered. In our in vitro model, lipotoxic insult diminished Akt activation and glucose uptake of HepG2 cells (Fig. 5D and F), with E2 preventing these effects. To further evaluate insulin resistance, phosphoenolpyruvate carboxykinase (PEPCK) activity was measured in liver of HFD male and female rats. Insulin stimulation decreased PEPCK activity in all animal groups (Fig. 5G). In

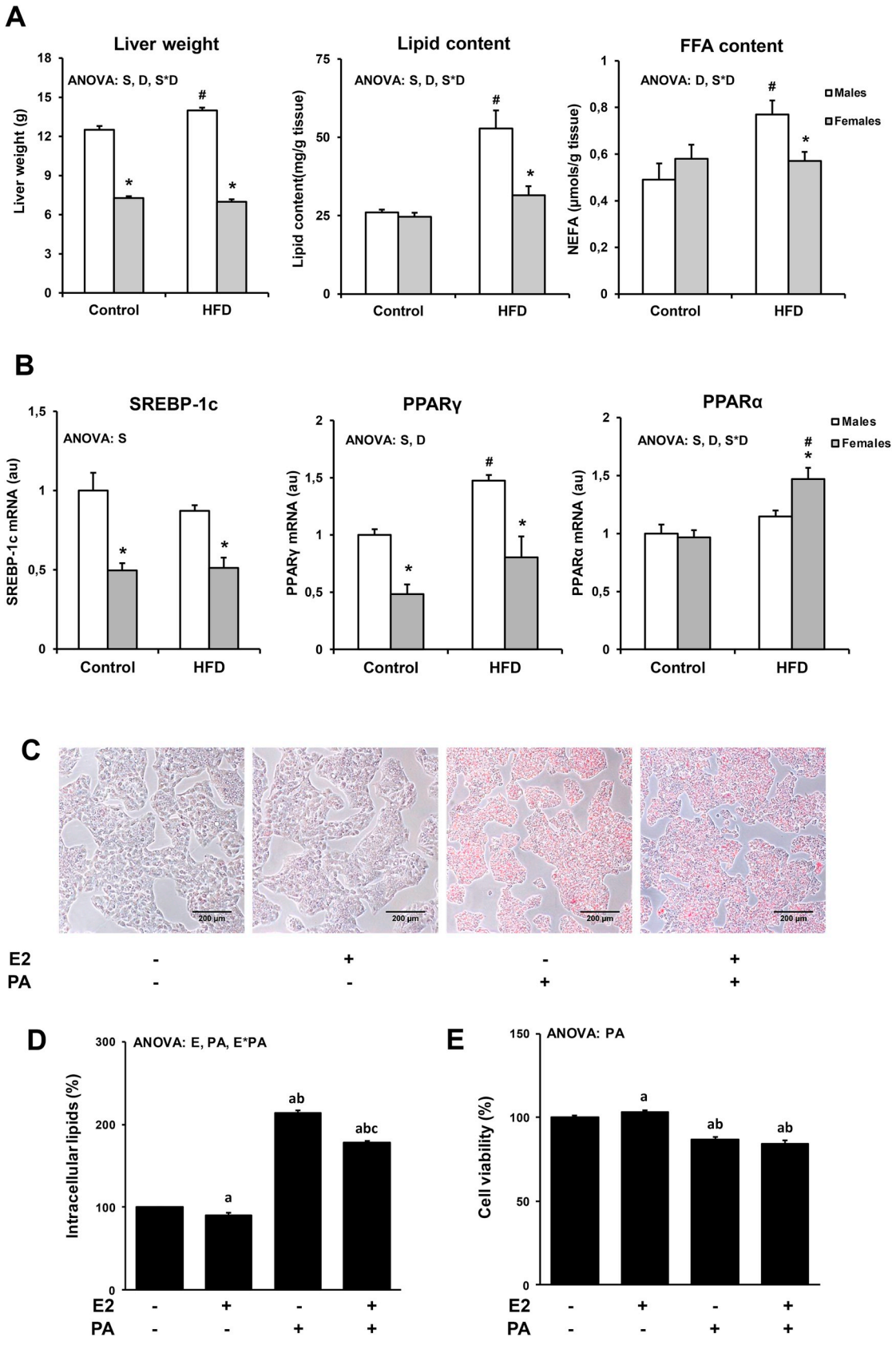


*(caption on next page)*

**Fig. 2.** Lipid accumulation and expression of master regulators of lipid metabolism in liver of HFD rats and HepG2 cells treated with E2 and PA. A) Weight, total lipid and FFA content in liver of HFD rats. B) Expression levels of SREBP-1c, PPARγ and PPARα in liver of HFD rats. Values are expressed as the mean ± SEM of 7 animals per group. ANOVA ($P < 0.05$): S, sex effect; D, diet effect; S*D, sex and diet interactive effect. Student's t-test ($P < 0.05$): * male vs. female; # HFD vs. control. C) Representative Oil Red O staining for HepG2 cells treated with PA (0.75 mM) and/or E2 (100 nM) or vehicle (ethanol) for 24 h. Control cells were treated with PA vehicle (BSA). Microscopy images were obtained at 100X magnification. D) Colorimetric quantification of Oil Red O staining after solubilization of the dye. E) Cell viability analysed by crystal violet assay. E2, 17β-estradiol; PA, palmitate. Values are expressed as the mean ± SEM of three independent experiments performed in duplicate ($n = 6$). ANOVA ($P < 0.05$): E, E2 effect; PA, PA effect; E*PA, E2 and PA interactive effect. Student's t-test ($P < 0.05$): *a* vs. control (*E2 − PA −*), *b* vs. *E2 +*, *c* vs *PA +*.

comparison with male rats, PEPCK activity was lower in females in both non-stimulated and stimulated insulin conditions. Moreover, the ability of insulin to repress PEPCK activity (striped bars in Fig. 5G), was impaired by HFD in male rats (34 vs 13 repression percentage for control and HFD-fed male rats, respectively), while it was unaltered in female rats (27 vs 28% for control and HFD-fed female rats, respectively). In HepG2 cells (Fig. 5H), PEPCK levels increased in response to PA, with E2 once again preventing this alteration.

To confirm the involvement of ROS and JNK activation in the E2-protective effect under lipotoxic conditions, HepG2 cells were treated with the JNK inhibitor SP600125 and the ROS-scavenger butylated hydroxyanisole (BHA) in the presence of PA and E2. As shown in Fig. 6, both SP600125 and BHA were effective to alleviate PA-induced JNK phosphorylation at same levels as E2 (Fig. 5B). In addition, simultaneous treatment with E2 and SP600125 showed similar effect than individual treatments (Fig. 6A). HepG2 fat accumulation showed a similar profile (Fig. 6B), suggesting that the effects of E2 preventing lipid accumulation are not independent of JNK inhibition or ROS scavenging.

## 3. Discussion

In the present study, we describe a role for E2 in maintaining insulin sensitivity in PA-induced lipotoxicity in HepG2 cells. This hormonal effect is associated with lower activation of JNK, one of the main drivers of insulin resistance, by means of an improvement in mitochondrial function and reduction of ROS production. These findings support the sexual dimorphism found in the systemic and hepatic insulin resistance induced by HFD feeding, in which male rats show a worsened profile compared to females.

Our results point to more deleterious effects of HFD feeding on systemic insulin sensitivity in male rats compared to females. In fact, serum lipid levels and insulin resistance markers were significantly higher in our HFD male rats, whereas females were almost unaffected. It is well described in most rodent models that females are more protected against HFD-induced insulin resistance than males [14,25,26]. As an example, Zucker Diabetic Fatty (ZDF) male rats on normal rodent chow diet develop hyperglycaemia and hypoinsulinaemia by 4 months of age, whereas female ZDF rats maintain normal glucose and insulin levels throughout their life, even at similar degree of obesity. This sex difference also translates to humans, with women less prone to suffer from diet-induced complications of T2DM and being less frequently diagnosed than men [27,28].

In this study, HFD-fed male rats showed hepatic steatosis, the hallmark of NAFLD. This process could be the result of both increased FFA flux into the circulation and subsequent uptake of fatty acids into the liver, as well as altered levels of proteins involved in lipid handling. In fact, increased levels of PPARγ and SREBP-1c, both associated to the development of hepatic steatosis [29], were higher in control and HFD-fed male compared to female rats. In contrast, PPARα, which is known to promote fatty acid oxidation [30], was increased only in female rats in response to HFD feeding. Along these lines, the SREBP-1c/PPARα ratio, which has been used as an index of steatosis in liver [31], is significantly lower in female compared to male rats when both are fed a HFD (0.57 ± 0.08 vs 0.95 ± 0.13, $P < 0.05$). Thus, female rats express a transcription factor signature more given to a higher hepatic rate of fatty acid oxidation, in contrast to the more lipogenic signature of males, protecting females against excessive lipid accumulation in liver.

Liver steatosis is associated with both hepatic and systemic insulin resistance [32,33]. In our study, only HFD male rats showed an impaired response to insulin in liver. Female rats, however, maintained insulin dependent Akt activation and PEPCK repression in liver despite HFD feeding. In this sense, previous studies have shown that ovariectomy impairs hepatic PI3K/Akt signalling pathway in rats, which this impairment reversed by E2 supplementation [34] Studies of ERα and ERβ knockout mice have demonstrated that ERα, but not ERβ gene depletion, results in increased glucose intolerance and insulin resistance [35]. The importance of E2/ERα axis in liver insulin sensitivity has been observed even in males, with mice lacking liver estrogen receptor α (LERKO) or lacking E2 by aromatase knockdown (ARKO mice) showing impaired glucose tolerance [36,37]. On the other hand, studies of G protein-coupled estrogen receptor 1 (GPER) knockout mice have revealed functions for GPER in the regulation of obesity, insulin resistance and glucose intolerance [38]. Interestingly, only female GPER KO mice exhibited increased lipid accumulation in liver along with a decrease in circulating HDL levels compared to wild type mice, whereas male mice displayed no such differences [39]. Altogether, *in vivo* studies suggest both ERα and GPER as candidates in mediating the estrogen protective effects observed in females.

To elucidate the contribution of E2 in ameliorating hepatic alterations associated to HFD feeding, experiments using HepG2 cells under lipotoxic PA concentrations were performed. Thus, PA exposure increased lipid content and reduced insulin sensitivity, accompanied by increased PEPCK expression, indicative of the inability of insulin to suppress gluconeogenesis. E2 attenuated hepatic steatosis and maintained insulin sensitivity in PA-treated cells, supporting the protective role suggested for estrogenic signalling.

JNK is one of the most investigated links between lipotoxic insult and development of insulin resistance in liver [19,40]. Among the mechanisms proposed, the activation of JNK induces IRS1 phosphorylation at serine 307, and subsequently impairs insulin signalling in the liver, as observed in HFD fed mice and PA-exposed hepatocytes [41–43]. Consistent with this, in our study HFD and PA exposure increased JNK activation in rats and HepG2 cells, respectively. Remarkably, both control and HFD-fed female rats exhibited lower JNK activation compared to their male counterparts. Similarly, JNK activation was lower in HepG2 cells treated with E2, even in the absence of PA. These results suggest than E2 could contribute to maintaining hepatic insulin sensitivity through a decrease in JNK activation, not only under lipotoxic conditions, but also under standard feeding conditions.

In order to identify mechanisms involved in the protective effect of E2, through a lower JNK activation, we evaluated mitochondrial function and oxidative stress. Inefficient fatty acid oxidation in mitochondria and increased oxidative damage are features of NAFLD [44,45]. In fact, sustained JNK activation requires a feed-back loop involving mitochondria and ROS [21]. Activated JNK interacts with the outer mitochondrial membrane protein, SH3 domain–binding protein 5 (SAB), resulting in impaired mitochondrial respiration and ROS release [46]. In turn, through a thioredoxin dependent mechanism, ROS trigger a cascade of kinases resulting in further activation of JNK [47]. The duration and degree of sustained JNK activation mediates many consequences, both through transcriptional regulation by AP-1 targets that

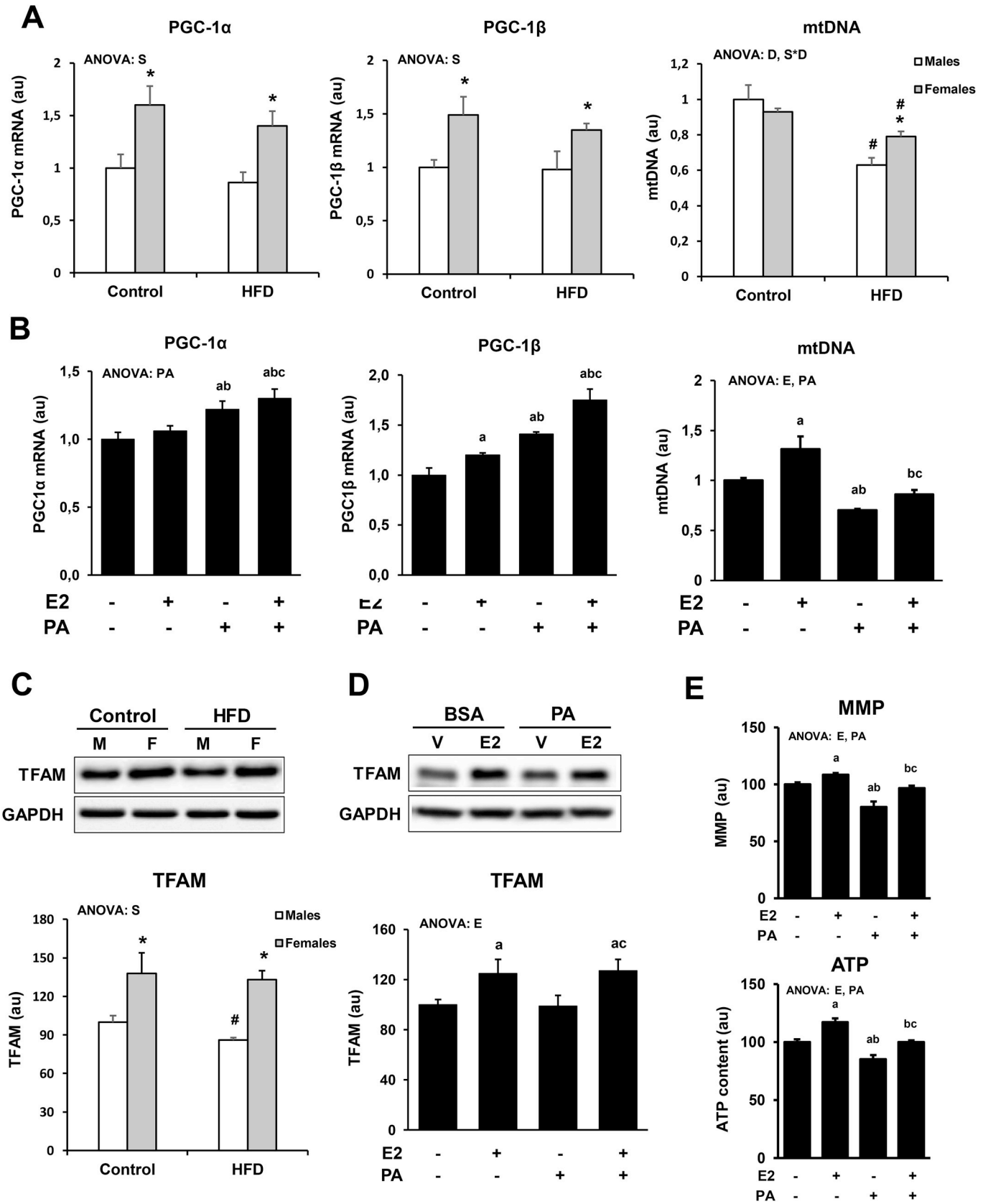


**Fig. 3.** Mitochondrial biogenesis and function in liver of HFD-fed male and female rats and in HepG2 cells treated with PA and E2. Expression levels of PGC1-α, PGC1-β and levels of mtDNA in liver (A) and HepG2 cells treated with PA and/or E2 (B). Representative bands and protein levels of TFAM in liver (C) and HepG2 cells (D). E) MMP and ATP content levels in HepG2 cells treated with PA and/or E2. Values are expressed as the mean ± SEM of three independent experiments performed in duplicate ($n = 6$). ANOVA ($P < 0.05$): E, E2 effect; PA, PA effect; E*PA, E2 and PA interactive effect. Student's t-test ($P < 0.05$): *a* vs. control (*E2 −* *PA −*), *b* vs. *E2 +*, *c* vs *PA +*.

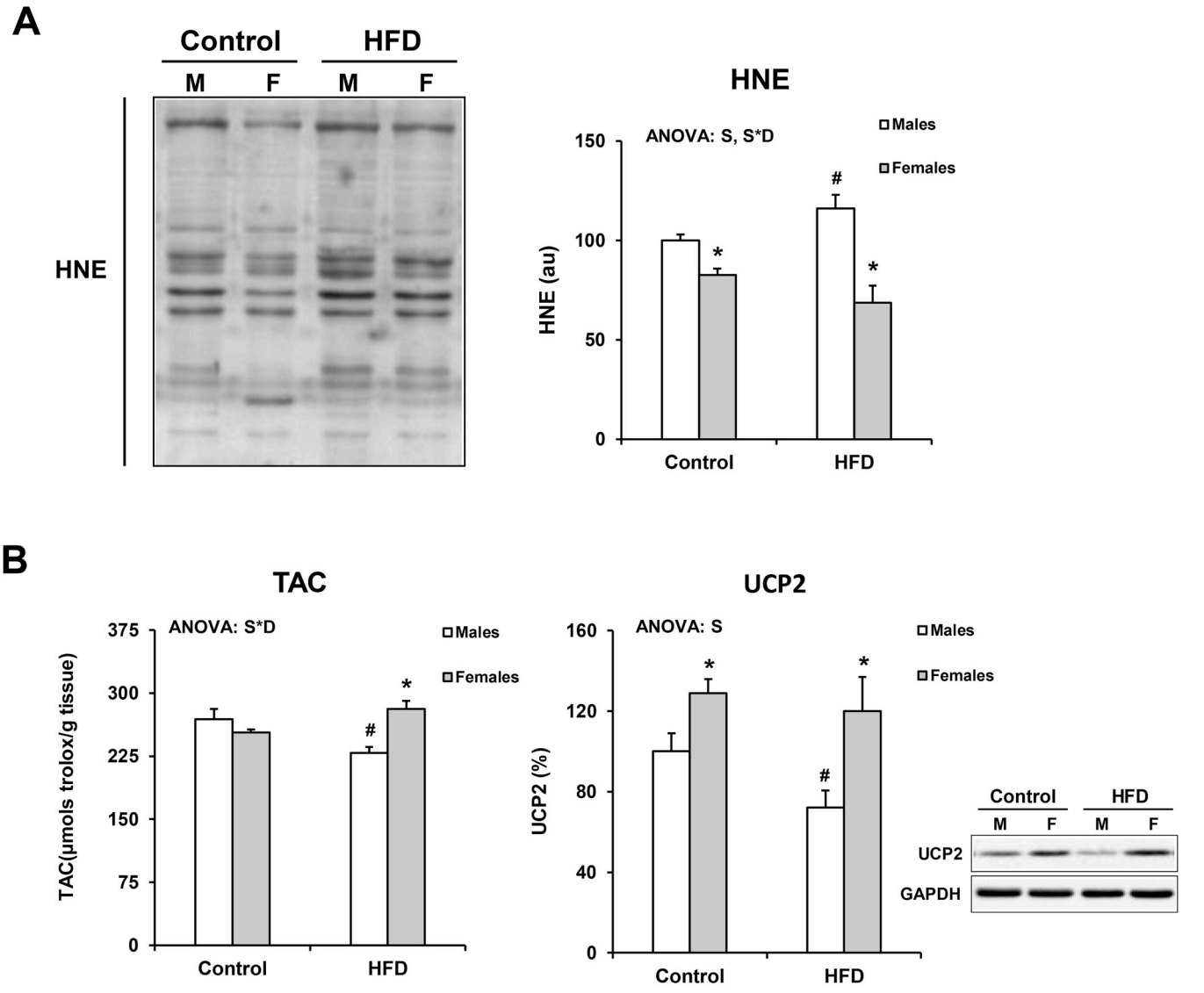


*(caption on next page)*

**Fig. 4.** Markers of oxidative stress and antioxidant capacity in liver of HFD-fed male and female rats and in HepG2 cells treated with PA and E2. A) Representative western blot of 4-HNE protein adducts in liver samples. Histograms are means, and bars are SEM of total 4-HNE protein adducts. B) Total antioxidant capacity (TAC) measured by colorimetric assay and UCP2 protein levels measured by western blot in liver of HFD rats. Representative western blot bands are shown. Values are expressed as the mean ± SEM of 7 animals per group. ANOVA ($P < 0.05$): S, sex effect; D, diet effect; S*D, sex and diet interactive effect. Student's t-test ($P < 0.05$): * male vs. female; # HFD vs. control. C) Antioxidant MnSOD and catalase levels quantified by western blot in HepG2 cells treated with PA and/or E2. D) ROS content measured by DCFH-DA method in HepG2 cells exposed to PA and/or E2. Values are expressed as the mean ± SEM of three independent experiments performed in duplicate ($n = 6$). ANOVA ($P < 0.05$): E, E2 effect; PA, PA effect; E*PA, E2 and PA interactive effect. Student's t-test ($P < 0.05$): *a* vs. control (*E2 −PA −*), *b* vs. *E2 +*, *c* vs *PA +*. HFD, high fat diet; M, male; F, female; UCP2, uncoupling protein 2; GAPDH, glyceraldehyde 3-phosphate dehydrogenase; HNE, 4-hydroxynonenal; E2, 17β-estradiol; V, vehicle; PA, palmitate; MnSOD, manganese superoxide dismutase.

modulate expression of many genes involved in proliferation, inflammation, metabolism and apoptosis (reviewed in Ref. [22]).

Considering this activation loop, one possible mechanism for dampening sustained activation of JNK by E2 may be targeting mitochondria. This idea is supported by our previous study showing an improvement in mitochondrial biogenesis and function in liver of OVX + E2 rats and in HepG2 supplemented with E2 [18]. In line with this, HFD male rats showed a significant decrease in the main markers of mitochondrial function, accompanied by an increase in oxidative stress. In fact, antioxidant systems failed in male rats, contributing to greater lipid oxidative damage. These findings are supported by data obtained in HepG2 cells, in which PA treatment impaired mitochondrial function and elevated ROS content, whereas E2 supplementation counteracted these effects. Besides improving mitochondrial function, E2 also enhance mitochondrial antioxidant defences such as MnSOD and UCP2. Among them, UCP2 may contribute to hepatoprotective role against steatosis and oxidative damage by mediating proton leak across the inner membrane avoiding ROS production and enhancing fatty acid oxidation. Although mitochondria have been widely reported to be an important target of E2 action, it cannot be ruled out the involvement of other pathways converging in JNK activation. For instance, PA oversupply has been reported to induce endoplasmic reticulum (ER) stress resulting in JNK activation [48] and thus, further research would be necessary to address whether E2 could be also acting through a mitigation of ER stress.

Estrogenic improvement of mitochondrial function and decrease in both ROS production and JNK activation could meaningfully alleviate progression of hepatic insulin resistance. Our results are not only in accordance with JNK inhibition strategies to mitigate insulin resistance and associated abnormalities [20,40,41], but also with therapies directly targeting mitochondria to halt or reverse the progression of liver diseases [45]. In fact, treatment with the JNK inhibitor SP600125 or the antioxidant BHA had no additive effects over those exerted by E2, showing interdependence between ROS, JNK activation and the putative E2-target. In a recent study, Win et al. elegantly demonstrated that female mice have lower expression of the mitochondrial protein SAB, showing a higher protection against acetaminophen-induced liver injury compared to males [49]. Although we have not assessed the expression of SAB in this study, our results are consistent and complementary with those of Win et al., suggesting a pleiotropic action of E2 on mitochondria beyond the lower expression of this docking protein, through improvement of mitochondrial biogenesis, function, antioxidant defences and fatty acid oxidation. The remodelling of all these features by E2 would set the threshold and amplification capacity of the sustained JNK activation loop, to levels aimed to protect females against lipotoxic insults in liver.

Altogether, our results depict a role for E2 against lipid-induced insulin resistance by targeting liver mitochondrial metabolism at different levels, which, in turn, attenuates ROS production and subsequently disrupts the sustained JNK activation loop. This study contributes to the understanding of sexual dimorphism in the incidence of NAFLD and associated alterations, which has been underestimated by the systematic use of male models.

## 4. Materials and methods

### 4.1. Animals and diets

All procedures performed in studies involving animals were in accordance with general guidelines approved by Institutional Ethics Committee (nr.3515/2012) and EU regulations (2010/63/UE). Six-week-old Wistar rats of both sexes were purchased at Charles River Laboratories (Barcelona, Spain) and housed in a controlled environment (22 °C and 65 ± 3% humidity) under a 12-h light-darkness cycle with free access to food and water. After 2 weeks of acclimation, animals were divided into 4 groups (n = 7): control males, control females, high fat diet (HFD) males and HFD females. All animals were fed ad libitum with a standard diet (control groups) or a high fat/high sucrose diet (HFD groups) for 16 weeks. Diets were delivered by SAFE (Paris, France). Standard diet used was SAFE 210 (3438 kcal/kg; 22.8% proteins, 13.1% lipids, and 64.1% carbohydrates) and HFD diet was SAFE 235 (4397 kcal/kg; 15.6% proteins, 46% lipid, and 38.5% carbohydrates). In order to analyse insulin response, comparable groups of animals fed control ($n = 7$) and high fat/high sucrose ($n = 7$) diets were treated with a peritoneal injection of insulin (5 U/kg body weight) 20 min before sacrifice. Non-stimulated animals received an equal volume of saline (0.9% NaCl). The estrous cycle was regularly determined by measuring vaginal wall impedance with the estrous cycle monitor Impeast® (Cibertec, Madrid, Spain) and confirmed by microscopic examination of fresh vaginal smears. All female rats were in the diestrous phase at the time of sacrifice. At 24 weeks of age, animals were decapitated without the use of anaesthetics to avoid metabolism alterations [50]. Blood was collected from the neck, and TG and glucose were determined using Accutrend® GCT-meter (Roche Diagnostics, Basilea, Switzerland). Blood was allowed to clot for 20min and was then centrifuged (1000 × *g*, 20 min, 4 °C) to obtain serum that was aliquoted and stored at −20 °C until analysis. The liver was quickly removed, placed in ice-cold saline solution, frozen in liquid nitrogen, and stored at −80 °C until analysis.

### 4.2. Glucose tolerance test

Glucose tolerance test was performed 4 days prior to sacrifice. Rats were fasted overnight and blood glucose levels were measured over a period of 120 min from the saphenous vein before and after glucose injection (2 g/kg body weight, intraperitoneal administration), using commercial test strips and an Accutrend® GCT-meter (Roche Diagnostics).

### 4.3. Serum parameters

ELISA kit was used to determine insulin levels (Mercodia, Uppsala, Sweden). FFA levels were measured using a colorimetric assay (Wako Chemicals GmbH, Neuss, Germany). The HOMA-IR (homeostasis model assessment of insulin resistance) index was calculated as [fasting serum glucose x fasting serum insulin/22.5].

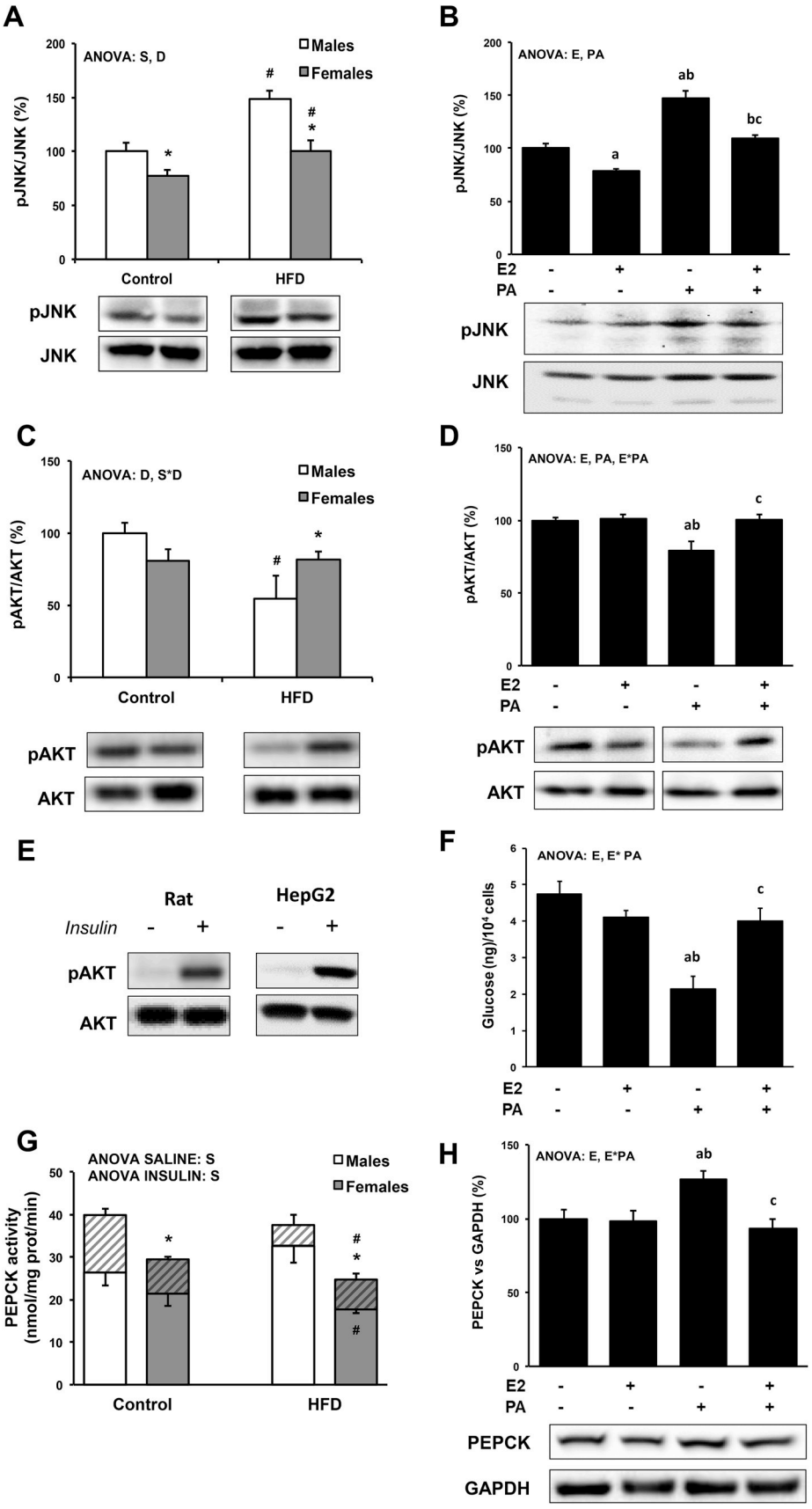


**Fig. 5.** JNK activation and insulin resistance in liver of HFD-fed male and female rats and in HepG2 cells treated with PA and E2. Representative western blots of p-JNK/JNK and p-Akt/Akt in HFD rats (A, C) and HepG2 cells (B, D). Akt protein levels were normalized to total Akt, and values of control male group or control group without E2 were set as 100. Animals were administered insulin (5 U/kg) 20 min before sacrifice. HepG2 cells were treated with PA (0.75 mM) combined with E2 (100 nM) or the vehicle (ethanol) for 24 h. Control cells were treated with PA vehicle (BSA and NaOH), and Akt pathway was assessed after 10 nM insulin stimulation for 15min. HFD, high fat diet; E2, 17β-estradiol; PA, palmitate. *In vivo*, values are expressed as the mean ± SEM of 7 animals per group. E) Representative bands of p-AKT induction by insulin in control rat and HepG2 cells. F) Glucose consumption in HepG2 cells. PEPCK activity in liver (G) and HepG2 cells (H). Sum of solid and striped bars represent PEPCK activity of non-stimulated insulin animals, solid bars represent that of stimulated insulin animals. Stimulated insulin animals were administered insulin (5 U/kg) 20 min before sacrifice. Values are expressed as the mean ± SEM of 7 animals per group. ANOVA ($P < 0.05$): S, sex effect; D, diet effect; S*D, sex and diet interactive effect. Student's t-test ($P < 0.05$): * male vs. female; # HFD vs. control. *In vitro*, values are expressed as the mean ± SEM of three independent experiments performed in duplicate ($n = 6$). ANOVA ($P < 0.05$): E, E2 effect; PA, PA effect; E*PA, E2 and PA interactive effect. Student's t-test ($P < 0.05$): *a* vs. control (*E2 − PA −*), *b* vs. *E2 +*, *c* vs *PA +*.

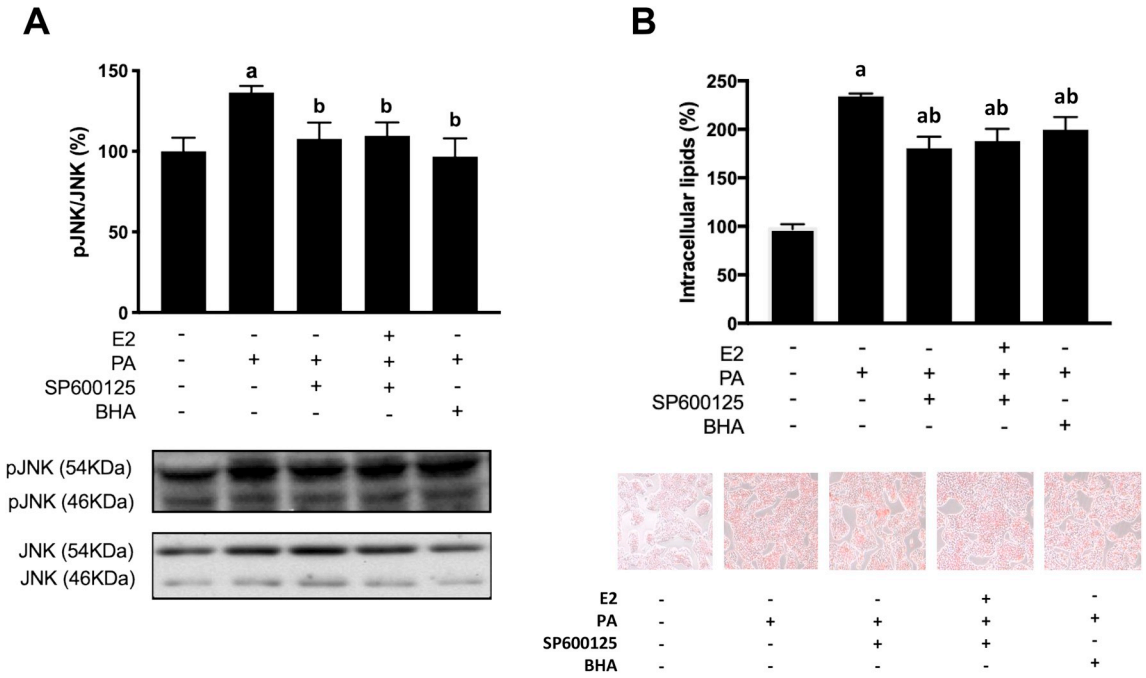


**Fig. 6.** JNK activation and lipid accumulation in HepG2 cells treated with PA and/or E2 after JNK inhibition and antioxidant treatment. A) pJNK protein levels were normalized to total JNK, and values of control male group were set as 100. Cells were treated with PA (0.75 mM) combined with E2 (100 nM), JNK inhibitor SP600125 (50 μM) or the ROS scavenger BHA (50 μM) for 24 h. Representative western blots are shown. B) HepG2 cells treated as in A) were analysed for lipid accumulation by Oil Red O staining. Histograms show colorimetric density after normalisation for cell density (crystal violet). Representative microscopic images are shown. Control cells were treated with PA vehicle (BSA). HFD, high fat diet; E2, 17β-estradiol; PA, palmitate; JNK, c-Jun-N-terminal kinase. Data are expressed as the mean ± SEM of three independent experiments performed in duplicate ($n = 6$). Student's t-test ($P < 0.05$): *a* vs. control (*E2 − PA −*), *b* vs. *PA +*.

### 4.4. Liver sample preparation and determinations

Total lipid content was quantified by the Folch method [51] and FFA levels fluorometrically using a kit from Sigma-Aldrich (St. Louis, MO, USA). A piece of liver was homogenized with a disperser (IKA T10 basic ULTRA-TURRAX) in a proportion of 0.1 g in 1 mL of STE buffer (250 mM sucrose, 20 mM Tris-HCl, 40 mM KCl, 2 mM EDTA, pH 7.4) and used for following determinations. TAC was measured using colorimetric assay kit (BioVision, San Francisco Bay Area, CA, USA). PEPCK activity was assessed spectrophotometrically as previously described [52]. The remaining volume was stored at −20 °C with phosphatase and protease inhibitors (1 mM sodium orthovanadate, 1 mM PMSF, 10 μM leupeptin, and 10 μM pepstatin) until Western blot analysis. Protein concentration was determined by the Bradford method [53].

### 4.5. HepG2 cell culture and treatments

Human hepatocellular carcinoma cell line HepG2 (American Type Culture Collection, Manassas, VA, USA) was routinely maintained at 37 °C in a humidified atmosphere of 5% $CO_2$ in MEM containing 5.6 mM glucose (Biowest, Nuaillé, France), supplemented with 10% fetal bovine serum (FBS) and 1% penicillin-streptomycin, from Biowest and Biological Industries (Beit-Haemek, Israel) respectively. All experiments were conducted between ninth and fourteenth passages. HepG2 cells ($4 \times 10^5$) were seeded in 6-well plates until 70% confluence and pretreated with phenol-red-free MEM 5.6 mM glucose (Biological Industries) supplemented with 10% charcoal-stripped FBS (Biological Industries) and 1% penicillin-streptomycin 24 h before treatments. Afterwards, cells were treated with 0.75 mM PA in combination with 100 nM E2, 50 μM SP600125, 50 μM BHA or vehicle (0.0002% ethanol), for 24 h. The dose of E2 used in this study is based on our preliminary dose curve analysis and is commonly used in HepG2 cells [54,55]. To study the insulin pathway, parallel experiments were carried out with 10 nM insulin stimulation for 15min. Preliminary experiments were carried out to determine the appropriate concentration of each compound, and cell viability was assessed in 96-well plates using crystal violet nuclear staining assay [56]. Briefly, cells were stained with 0.5% (w/v) crystal violet in 30% (v/v) acetic acid for 10min. After washing, the dye was solubilized in 100 μL of methanol and absorbance was measured photometrically at 595 nm to determine cell viability.

PA-albumin complex preparation was performed by saponification. Briefly, 50 mM of PA was preheated in 0.1 N NaOH at 70 °C for 15 min. Then, the solution was conjugated at 37 °C for 30 min with MEM containing fatty-acid-free BSA to make a 5 mM working stock at a molar ratio of PA:BSA 4:1. Control cells were treated with BSA and NaOH, in final concentrations of 1.2% and 1.5 mM, respectively.

For Western blot analysis, $4 \times 10^5$ cells were seeded in 6-well plates and treated as previously described. After treatment, cells were washed twice with PBS and scrapped in 0.15 mL of ice-cold RIPA buffer (50 mM Tris pH 7.5, 1% Triton X-100, 1 mM EDTA, 150 mM NaCl, 0.5% sodium deoxicolate, and 0.1% SDS) containing phosphatase and protease inhibitors (10 μM leupeptin, 10 μM pepstatin, 10 μM PMSF, 1 mM NaF, and 1 mM $Na_3VO_4$). Cell lysate extracts were scraped off, vortex-mixed, and centrifuged (14,000×*g*, 10 min, 4 °C). Protein concentration was determined by the bicinchoninic acid method (Thermo Fisher Scientific, Waltham, MA, USA).

### 4.6. PCR and mitochondrial DNA levels

Total RNA was obtained from 0.1 g of liver or ~$5 \times 10^5$ HepG2 cells using TriPure® Isolation Reagent (Roche Diagnostics), following the manufacturer's instructions. About 1 μg of total RNA was reverse transcribed to cDNA using 25U MuLV reverse transcriptase in 10 μl retrotranscription mixture (10 mM Tris-HCl pH 9.0, 50 mM KCl, 0.1% Triton X-100, 2.5 mM $MgCl_2$, 2.5 μM random hexamers, 10 U/μL RNase inhibitor and 500 μM of each dNTP) for 60 min at 42 °C in a Gene Amp

9700 thermal cycler (Applied Biosystems, Waltham, MA, USA). cDNA solutions were diluted 1/10 and aliquots were frozen at −20 °C until analysed. Real-time PCR was performed using LightCycler®480 SYBR Green I Master Technology in a LightCycler® 480 System II rapid thermal cycler (Roche Diagnostics). Each reaction contained 5 μL of LightCycler®480 SYBR Green I master (containing FastStart Taq DNA polymerase, dNTP mix, reaction buffer, $MgCl_2$ and SYBR Green I dye), sense and antisense primers (0.374 μM each), and 2.5 μL of the cDNA dilution in a final volume of 10 μL. The amplification program consisted of a pre-incubation step for denaturation of template DNA (95 °C, 2min), followed by 40 cycles consisting of a denaturation (95 °C, 5min), annealing (primer-dependent temperature, 10 s), and extension steps (72 °C, 12s). Glyceraldehyde 3-phosphate dehydrogenase (GAPDH) was used as a housekeeping gene in all expression analyses.

To determine mtDNA levels, total DNA from the liver was obtained using a DNA extraction kit (Roche Diagnostics), whereas total DNA from HepG2 cells was obtained using TriPure® Isolation Reagent (Roche Diagnostics). Real-time PCR was performed as above, and each reaction contained 5 μL of LightCycler®480 SYBR Green I master, sense and antisense primers (0.374 μM each), and 5 ng of the isolated DNA in a final volume of 10 μL. The mitochondrial gene NADH dehydrogenase subunit ND4 was used for semi-quantification of mtDNA, and the nuclear gene GAPDH was used for normalisation.

Annealing temperature was 60 °C for all the primers used. Oligonucleotide sequences and product length in real-time PCR are detailed in Table 1. After each cycle, fluorescence was measured at 72 °C. Product specificity was confirmed in initial experiments by agarose gel electrophoresis and routinely by melting curve analysis.

### 4.7. Oil red O staining

Oil Red O was used to stain intracellular lipids. HepG2 cells ($2 \times 10^5$) were seeded in 12-well plates and treated with PA and E2 as mentioned above. Then, HepG2 cells were fixed in 10% phosphate-buffered formalin for 1 h and stained with 2.1 mg/mL Oil Red O in 60% isopropanol for 10 min. Excess stain was removed by washing with distilled water and cell images were then obtained using an inverted Eclipse TS100-F microscope (Nikon, Tokyo, Japan) connected to a Nikon D80 camera (Nikon). Stained oil droplets were dissolved with 0.5 mL isopropanol and absorbance of dye-triglyceride complex was measured at 500 nm. Values were normalized per number of viable cells determined by crystal violet nuclear staining assay [56].

#### 4.7.1. Glucose consumption

The glucose consumption was estimated by the method described by Li et al. [57] with some modifications. HepG2 cells were seeded in 96-well plates at a density of $1.5 \times 10^4$ cells/well with eight wells left as blanks. Cells were treated with PA and E2 for 24 h as detailed above. The medium was removed 24 h later and glucose concentration was estimated using a commercial kit (Cromatest, Linear Chemicals, Spain). Consumption was calculated by the glucose concentrations of blank wells minus glucose concentrations in plated wells. The CV assay was used to adjust the glucose consumption. There were eight replicates for each treatment and the experiment was repeated twice.

### 4.8. Western blot analysis

Fifty μg of protein from hepatic homogenates and from HepG2 cell lysates were fractioned on SDS-PAGE gels and electrotransferred into a nitrocellulose membrane. The membranes were blocked (5% non-fat powdered milk in TBS, pH 7.5, containing 0.05% Tween 20) for 1 h and incubated overnight with the corresponding primary antibody. Antibodies for Akt (60 kDa), pAkt (Ser473), JNK (46/54 kDa), pJNK (Thr183/Tyr185), and human TFAM (24 kDa) were supplied by Cell Signaling (Danvers, MA, USA); antibodies against PEPCK (62 kDa), MnSOD (25 kDa), UCP2 (35 kDa), 4-hydroxynoneal (HNE; used as a lipid oxidative damage marker), and GAPDH (37 kDa; used as the loading control) were purchased from Santa Cruz Biotechnology (Santa Cruz, CA, USA); anti-catalase (60 kDa) was from Merck-Millipore; while antibody against rat TFAM was kindly provided by Dr H Inagasaki. Development of immunoblots was performed using Clarity Western Chemiluminescence kit (Bio-Rad, Hercules, CA, USA). Protein bands were detected using the ChemiDoc XRS System (Bio-Rad) and analysed using the image analysis program Quantity One 1-D (Bio-Rad). Precision Plus Protein Dual Color Standard (Bio-Rad) was used as a molecular weight marker.

### 4.9. Mitochondrial membrane potential, and ATP and ROS content

For all determinations, $1.5 \times 10^4$ HepG2 cells were seeded in 96-well plates and treated with PA and E2 as detailed above. Values were normalized per number of viable cells determined by crystal violet nuclear staining assay [56]. MMP was tested using tetramethylrhodamine methylester (TMRM) as a lipophilic cationic dye that accumulates within mitochondria according to the membrane potential [58]. Cells were dyed with 0.5 μM of TMRM for 15 min at 37 °C in darkness, and fluorescence measurement was performed in an FLx800 96-well microplate reader (BioTek, Winooski, VT, USA) with excitation at 552 nm and emission at 576 nm. ATP was measured with an ATP bioluminescent assay kit (BioVision) following the manufacturer's instructions. Finally, generation of intracellular ROS was determined by the 2',7'-dichlorofluorescin diacetate (DCFH-DA) method [59]. Cells

**Table 1**
Oligonucleotide primer sequences used in real-time PCR amplification and product length.

| Gene | Forward primer (5'→3') | Reverse primer (5'→3') | Accession Number | Product length (bp) |
|---|---|---|---|---|
| mtDNA (R) | TACACGATGAGGCAACCAAA | GGTAGGGGGTGTGTTGTGAG | NC_001665 | 162 |
| PGC-1α (R) | ATCTACTGCCTGGGGACCTT | ATGTGTCGCCTTCTTGCTCT | NM_031347 | 180 |
| PGC-1β (R) | ACTATGATCCCACGTCTGAAGAGTC | CCTTGTCTGAGGTATTGAGGTATTC | NM_176075 | 152 |
| PPARα (R) | TGCCTTCCCTGTGAACTGAC | GCTTCAAGTGGGGAGAGAGG | NM_013196.1 | 151 |
| SREBP-1c (R) | CGCTACCGTTCCTCTATCAATGAC | AGTTTCTGGTTGCTGTGCTGTAAG | NM_001276707.1 | 140 |
| PPARγ (R) | TCAGAGGGACAAGGATTCATGA | CACCAAAGGGCTTCCGCAGGCT | NM_013124 | 61 |
| GAPDH (R) | ACTTTGGCATCGTGGAAGGG | CCGTTCAGCTCTGGGATGAC | NM_017008.4 | 178 |
| mtDNA (H) | CCTGACTCCTACCCCTCACA | ATCGGGTGATGATAGCCAAG | NC_013993.1 | 198 |
| PGC-1α (H) | CACTCCTCCTCATAAAGCCAAC | GGACTTGCTGAGTTGTGCATA | NM_013261.5 | 190 |
| PGC-1β (H) | GCTGACAAGAAATAGGAGAGGC | TGAATTGGAATCGTAGTCAGTG | NM_133263.4 | 184 |
| GAPDH (H) | CTGGTGGTCCAGGGGTCTTA | CCACTCCTCCACCTTTGACG | NM_002046.7 | 156 |

R, rat; H, human; mtDNA, mitochondrial DNA; PGC-1α, peroxisome proliferator-activated receptor coactivator 1α; PGC-1β, peroxisome proliferator-activated receptor coactivator 1β; PPARα, peroxisome proliferator activated receptor α; SREBP-1c, sterol regulatory element binding transcription factor 1c; PPARγ, peroxisome proliferator-activated receptor gamma; GAPDH, glyceraldehyde 3-phosphate dehydrogenase.

were incubated for 45 min at 37 °C in darkness with 10 μM DCFH-DA, and fluorescence intensity was measured with excitation and emission wavelengths of 485 and 530 nm, respectively.

### 4.10. Statistical analysis

*In vivo* data are expressed as the mean ± SEM of 7 animals per group. Statistical differences between groups were analysed by two-way ANOVA with sex and diet as factors. Student's t-test was applied as a post hoc analysis. *In vitro* data were analysed from 3 individual experiments performed in duplicate ($n = 6$) and statistical differences between groups were assessed by two-way ANOVA for E2 and PA. Student's t-test was applied as a post hoc analysis. All statistical analyses were performed using a statistical software package (IBM SPSS 26.0 for Mac OSX), and a $P$ value $^{<}0.05$ was considered statistically significant. Threshold cycle (Ct) values of real-time PCR were analysed using GenEx Standard Software 5.3.6 (MultiD Analyses AB, Sweden), and the efficiency of the reaction was taken into account for each gene.

## Ethics approval and consent to participate

Not applicable.

## Consent for publication

Not applicable.

## Funding

This work was supported by FEDER / Ministerio de Ciencia, Innovación y Universidades. Agencia Estatal de Investigación (SAF2010-21792; SAF2016-80384R) of the Spanish Government; and by Comunitat Autònoma de les Illes Balears (PCTIB-31/2011, AAEE43/2014, AAEE52/2015). BM G-P was funded by a FPU grant from the Ministerio de Educación, Cultura y Deporte (AP2012-1004) of the Spanish Government. MR M-C and M S-R were funded by a grant from Balearic Islands Government (FPI/1888/2016 and FPI11-41523224J, respectively), after being selected in the framework on an operating program co-financed by the European Social Fund. M B-T was funded by a grant of University of Balearic Islands (07-2014-0303240). This work received a grant by the Health Research Institute of the Balearic Islands (IdISBa) to support open access publishing.

## Authors' contributions

ILL and MG designed of the work; BGP, MMC, MBT, AMC and MSR performed *in vivo* and in vitro experiments, acquisition of data and statistical analysis, AV, ILL, AMP and MG have interpreted the data, drafted the work and revised it.

## Declaration of competing interest

None.

## Acknowledgements

In ever loving memory of Professor García-Palmer.

## References

[1] M. Asrih, F.R. Jornayvaz, Metabolic syndrome and nonalcoholic fatty liver disease: is insulin resistance the link? Mol. Cell. Endocrinol. 418 (2015) 55–65, https://doi.org/10.1016/j.mce.2015.02.018.
[2] G. Boden, Obesity and free fatty acids, Endocrinol Metab. Clin. N. Am. 37 (2008) 635–646, https://doi.org/10.1016/j.ecl.2008.06.007.
[3] J. Yu, S. Marsh, J. Hu, W. Feng, C. Wu, The pathogenesis of nonalcoholic fatty liver disease: interplay between diet, gut microbiota, and genetic background, Gastroenterol. Res. Pract. 2016 (2016) 2862173, https://doi.org/10.1155/2016/2862173.
[4] A.L. Birkenfeld, G.I. Shulman, Nonalcoholic fatty liver disease, hepatic insulin resistance, and type 2 Diabetes, Hepatology 59 (2014) 713–723, https://doi.org/10.1002/hep.26672.
[5] P. Loria, A. Lonardo, F. Anania, Liver and diabetes. A vicious circle, Hepatol. Res. 43 (2012) 51–64, https://doi.org/10.1111/j.1872-034X.2012.01031.x.
[6] A.A. Gupte, H.J. Pownall, D.J. Hamilton, Estrogen: an emerging regulator of insulin action and mitochondrial function, J. Diabetes Res. 2015 (2015) 1–9, https://doi.org/10.1155/2015/916585.
[7] M. Hamaguchi, T. Kojima, A. Ohbora, N. Takeda, M. Fukui, T. Kato, Aging is a risk factor of nonalcoholic fatty liver disease in premenopausal women, World J. Gastroenterol. 18 (2012) 237–243, https://doi.org/10.3748/wjg.v18.i3.237.
[8] A. Tsuneto, A. Hida, N. Sera, M. Imaizumi, S. Ichimaru, E. Nakashima, S. Seto, K. Maemura, M. Akahoshi, Fatty liver incidence and predictive variables, Hypertens. Res. 33 (2010) 638–643, https://doi.org/10.1038/hr.2010.45.
[9] J.M. Clark, F.L. Brancati, A.M. Diehl, Nonalcoholic fatty liver disease, Gastroenterology 122 (2002) 1649–1657, https://doi.org/10.1016/j.bpg.2010.08.005.
[10] J.D. Browning, L.S. Szczepaniak, R. Dobbins, P. Nuremberg, J.D. Horton, J.C. Cohen, S.M. Grundy, H.H. Hobbs, Prevalence of hepatic steatosis in an urban population in the United States: impact of ethnicity, Hepatology 40 (2004) 1387–1395, https://doi.org/10.1002/hep.20466.
[11] J.J. Pan, M.B. Fallon, Gender and racial differences in nonalcoholic fatty liver disease, World J. Hepatol. 6 (2014) 274–283, https://doi.org/10.4254/wjh.v6.i5.274.
[12] E.B. Geer, W. Shen, Gender differences in insulin resistance, body composition, and energy balance, Gend. Med. 6 (2009) 60–75, https://doi.org/10.1016/j.genm.2009.02.002.
[13] J. Kuhl, A. Hilding, C.G. Östenson, V. Grill, S. Efendic, P. Bavenholm, Characterisation of subjects with early abnormalities of glucose tolerance in the Stockholm Diabetes Prevention Programme: the impact of sex and type 2 diabetes heredity, Diabetologia 48 (2005) 35–40, https://doi.org/10.1007/s00125-004-1614-1.
[14] A. Nadal-Casellas, A.M. Proenza, I. Lladó, M. Gianotti, Sex-dependent differences in rat hepatic lipid accumulation and insulin sensitivity in response to diet-induced obesity, Biochem. Cell. Biol. 90 (2012) 164–172, https://doi.org/10.1139/o11-069.
[15] S. Stöppeler, D. Palmes, M. Fehr, J.P. Hölzen, A. Zibert, R. Siaj, H.H.J. Schmidt, H.U. Spiegel, R. Bahde, Gender and strain-specific differences in the development of steatosis in rats, Lab. Anim. 47 (2013) 43–52, https://doi.org/10.1177/0023677212473717.
[16] G. Paradies, V. Paradies, F.M. Ruggiero, G. Petrosillo, Oxidative stress, cardiolipin and mitochondrial dysfunction in nonalcoholic fatty liver disease, World J. Gastroenterol. 20 (2014) 14205–14218, https://doi.org/10.3748/wjg.v20.i39.14205.
[17] J.-Q. Chen, P.R. Cammarata, C.P. Baines, J.D. Yager, Regulation of mitochondrial respiratory chain biogenesis by estrogens/estrogen receptors and physiological, pathological and pharmacological implications, Biochim. Biophys. Acta Mol. Cell Res. 1793 (2009) 1540–1570, https://doi.org/10.1016/j.bbamcr.2009.06.001.
[18] B.M. Galmés-Pascual, A. Nadal-Casellas, M. Bauza-Thorbrügge, M. Sbert- Roig, F.J. García-Palmer, A.M. Proenza, M. Gianotti, I. Lladó, 17β-estradiol improves hepatic mitochondrial biogenesis and function through PGC1B, J. Endocrinol. 232 (2017) 297–308, https://doi.org/10.1530/JOE-16-0350.
[19] G. Solinas, B. Becattini, JNK at the crossroad of obesity, insulin resistance, and cell stress response, Mol. Metab. 6 (2017) 174–184, https://doi.org/10.1016/j.molmet.2016.12.001.
[20] R. Singh, Y. Wang, Y. Xiang, K.E. Tanaka, W.A. Gaarde, M.J. Czaja, Differential effects of JNK1 and JNK2 inhibition on murine steatohepatitis and insulin resistance, Hepatology 49 (2009) 87–96, https://doi.org/10.1002/hep.22578.
[21] S. Win, T.A. Than, N. Kaplowitz, The regulation of JNK signaling pathways in cell death through the interplay with mitochondrial SAB and upstream post-translational effects, Int. J. Mol. Sci. 19 (2018), https://doi.org/10.3390/ijms19113657.
[22] S. Win, T.A. Than, J. Zhang, C. Oo, R.W.M. Min, N. Kaplowitz, New insights into the role and mechanism of c-Jun-N-terminal kinase signaling in the pathobiology of liver diseases, Hepatology 67 (2018) 2013–2024, https://doi.org/10.1002/hep.29689.
[23] E. Seki, D.A. Brenner, M. Karin, A liver full of JNK: signaling in regulation of cell function and disease pathogenesis, and clinical approaches, Gastroenterology 143 (2012) 307–320, https://doi.org/10.1053/j.gastro.2012.06.004.A.
[24] C. Rojas, B. Pan-Castillo, C. Valls, G. Pujadas, S. Garcia-Vallve, L. Arola, M. Mulero, Resveratrol enhances palmitate-induced ER stress and apoptosis in cancer cells, PloS One 9 (2014) e113929, https://doi.org/10.1371/journal.pone.0113929.
[25] A. Hevener, D. Reichart, A. Janez, J. Olefsky, Female rats do not exhibit free fatty acid-induced insulin resistance, Diabetes 51 (2002) 1907–1912, https://doi.org/10.2337/diabetes.51.6.1907.
[26] U.S. Pettersson, T.B. Waldén, P.-O. Carlsson, L. Jansson, M. Phillipson, Female mice are protected against high-fat diet induced metabolic syndrome and increase the regulatory T cell population in adipose tissue, PloS One 7 (2012) e46057, https://doi.org/10.1371/journal.pone.0046057.
[27] J. Logue, J.J. Walker, H.M. Colhoun, G.P. Leese, R.S. Lindsay, J.A. McKnight, A.D. Morris, D.W. Pearson, J.R. Petrie, S. Philip, S.H. Wild, N. Sattar, Scottish Diabetes Research Network Epidemiology Group, Do men develop type 2 diabetes at lower body mass indices than women? Diabetologia 54 (2011) 3003–3006, https://doi.org/10.1007/s00125-011-2313-3.
[28] A. Kautzky-Willer, J. Harreiter, G. Pacini, Sex and gender differences in risk, pathophysiology and complications of type 2 diabetes mellitus, Endocr. Rev. 37

(2016) 278–316, https://doi.org/10.1210/er.2015-1137.
[29] L.A. Videla, P. Pettinelli, Misregulation of PPAR functioning and its pathogenic consequences associated with nonalcoholic fatty liver disease in human obesity, PPAR Res. 2012 (2012) 1–14, https://doi.org/10.1155/2012/107434.
[30] M. Vacca, M. Allison, J.L. Griffin, A. Vidal-Puig, Fatty acid and glucose sensors in hepatic lipid metabolism: implications in NAFLD, Semin. Liver Dis. 35 (2015) 250–261, https://doi.org/10.1055/s-0035-1562945.
[31] P. Pettinelli, T. Del Pozo, J. Araya, R. Rodrigo, A.V. Araya, G. Smok, A. Csendes, L. Gutierrez, J. Rojas, O. Korn, F. Maluenda, J.C. Diaz, G. Rencoret, I. Braghetto, J. Castillo, J. Poniachik, L.A. Videla, Enhancement in liver SREBP-1c/PPAR-alpha ratio and steatosis in obese patients: correlations with insulin resistance and n-3 long-chain polyunsaturated fatty acid depletion, Biochim. Biophys. Acta 1792 (2009) 1080–1086, https://doi.org/10.1016/j.bbadis.2009.08.015.
[32] R.J. Perry, V.T. Samuel, K.F. Petersen, G.I. Shulman, The role of hepatic lipids in hepatic insulin resistance and type 2 diabetes, Nature 510 (2014) 84–91, https://doi.org/10.1038/nature13478.
[33] M. Kleinert, C. Clemmensen, S.M. Hofmann, M.C. Moore, S. Renner, S.C. Woods, P. Huypens, J. Beckers, M.H. de Angelis, A. Schürmann, M. Bakhti, M. Klingenspor, M. Heiman, A.D. Cherrington, M. Ristow, H. Lickert, E. Wolf, P.J. Havel, T.D. Müller, M.H. Tschöp, Animal models of obesity and diabetes mellitus, Nat. Rev. Endocrinol. 14 (2018) 140–162, https://doi.org/10.1038/nrendo.2017.161.
[34] Y. Wang, B. Li, W. Zhang, Y. Liu, P. Xue, J. Ma, Y. Li, Impaired PI3 K Akt expression in liver and skeletal muscle of ovariectomized rats, Endocrine 44 (2013) 659–665, https://doi.org/10.1007/s12020-013-9894-1.
[35] P.A. Heine, J.A. Taylor, G.A. Iwamoto, D.B. Lubahn, P.S. Cooke, Increased adipose tissue in male and female estrogen receptor-α knockout mice, Proc. Natl. Acad. Sci. U.S.A. 97 (2000) 12729–12734, https://doi.org/10.1073/pnas.97.23.12729.
[36] S. Qiu, J.T. Vazquez, E. Boulger, H. Liu, P. Xue, M.A. Hussain, A. Wolfe, Hepatic estrogen receptor α is critical for regulation of gluconeogenesis and lipid metabolism in males, Sci. Rep. 7 (2017), https://doi.org/10.1038/s41598-017-01937-4.
[37] K. Toda, A. Toda, M. Ono, T. Saibara, Lack of 17β-estradiol reduces sensitivity to insulin in the liver and muscle of male mice, Heliyon 4 (2018), https://doi.org/10.1016/j.heliyon.2018.e00772.
[38] G. Sharma, C. Hu, J.L. Brigman, G. Zhu, H.J. Hathaway, E.R. Prossnitz, GPER deficiency in male mice results in insulin resistance, dyslipidemia, and a proinflammatory state, Endocrinology 154 (2013) 4136–4145, https://doi.org/10.1210/en.2013-1357.
[39] L. Meoli, J. Isensee, V. Zazzu, C.S. Nabzdyk, D. Soewarto, H. Witt, A. Foryst-Ludwig, U. Kintscher, P.R. Noppinger, Sex- and age-dependent effects of Gpr30 genetic deletion on the metabolic and cardiovascular profiles of diet-induced obese mice, Gene 540 (2014) 210–216, https://doi.org/10.1016/j.gene.2014.02.036.
[40] G. Tuncman, J. Hirosumi, G. Solinas, L. Chang, M. Karin, G.S. Hotamisligil, Functional in vivo interactions between JNK1 and JNK2 isoforms in obesity and insulin resistance, Proc. Natl. Acad. Sci. U.S.A. 103 (2006) 10741–10746, https://doi.org/10.1073/pnas.0603509103.
[41] J. Hirosumi, G. Tuncman, L. Chang, C.Z. Görgün, K.T. Uysal, K. Maeda, M. Karin, G.S. Hotamisligil, A central role for JNK in obesity and insulin resistance, Nature 420 (2002) 333–336, https://doi.org/10.1038/nature01137.
[42] D. Gao, S. Nong, X. Huang, Y. Lu, H. Zhao, Y. Lin, Y. Man, S. Wang, J. Yang, J. Li, The effects of palmitate on hepatic insulin resistance are mediated by NADPH Oxidase 3-derived reactive oxygen species through JNK and p38MAPK pathways, J. Biol. Chem. 285 (2010) 29965–29973, https://doi.org/10.1074/jbc.M110.128694.
[43] C.S. Achard, D.R. Laybutt, Lipid-induced endoplasmic reticulum stress in liver cells results in two distinct outcomes: adaptation with enhanced insulin signaling or insulin resistance, Endocrinology 153 (2012) 2164–2177, https://doi.org/10.1210/en.2011-1881.
[44] A. Besse-Patin, M. Léveillé, D. Oropeza, B.N. Nguyen, A. Prat, J.L. Estall, Estrogen signals through peroxisome proliferator-activated Receptor−γ coactivator 1α to reduce oxidative damage associated with diet-induced fatty liver disease, Gastroenterology 152 (2017) 243–256, https://doi.org/10.1053/j.gastro.2016.09.017.
[45] C. Auger, A. Alhasawi, M. Contavadoo, V.D. Appanna, Dysfunctional mitochondrial bioenergetics and the pathogenesis of hepatic disorders, Front. Cell Dev. Biol. 3 (2015) 40, https://doi.org/10.3389/fcell.2015.00040.
[46] S. Win, T.A. Than, R.W.M. Min, M. Aghajan, N. Kaplowitz, c-Jun N-terminal kinase mediates mouse liver injury through a novel Sab (SH3BP5)-dependent pathway leading to inactivation of intramitochondrial Src, Hepatology 63 (2016) 1987–2003, https://doi.org/10.1002/hep.28486.
[47] S.G. Cho, Y.H. Lee, H.S. Park, K. Ryoo, K.W. Kang, J. Park, S.J. Eom, M.J. Kim, T.S. Chang, S.Y. Choi, J. Shim, Y. Kim, M.S. Dong, M.J. Lee, S.G. Kim, H. Ichijo, E.J. Choi, Glutathione S-transferase Mu modulates the stress-activated signals by suppressing apoptosis signal-regulating kinase 1, J. Biol. Chem. 276 (2001) 12749–12755, https://doi.org/10.1074/jbc.M005561200.
[48] S. Win, T.A. Than, B.H.A. Le, C. García-Ruiz, J.C. Fernandez-Checa, N. Kaplowitz, Sab (Sh3bp5) dependence of JNK mediated inhibition of mitochondrial respiration in palmitic acid induced hepatocyte lipotoxicity, J. Hepatol. 62 (2015) 1367–1374, https://doi.org/10.1016/j.jhep.2015.01.032.
[49] S. Win, R.W. Min, C.Q. Chen, J. Zhang, Y. Chen, M. Li, A. Suzuki, M.F. Abdelmalek, Y. Wang, M. Aghajan, F.W. Aung, A.M. Diehl, R.J. Davis, T.A. Than, N. Kaplowitz, Expression of mitochondrial membrane-linked SAB determines severity of sex-dependent acute liver injury, J. Clin. Invest. 129 (2019) 5278–5293, https://doi.org/10.1172/JCI128289.
[50] J.K. Saha, J. Xia, J.M. Grondin, S.K. Engle, J.A. Jakubowski, Acute hyperglycemia induced by ketamine/xylazine anesthesia in rats: mechanisms and implications for preclinical models, Exp. Biol. Med. 230 (2005) 777–784, https://doi.org/10.1177/153537020523001012.
[51] J. Folch, M. Lees, G.H.S. Stanley, A simple method for the isolation and purification of total lipides from animal tissues, J. Biol. Chem. 226 (1957) 497–509.
[52] L. Opie, E. Newsholme, The activities of fructose 1,6-diphosphatase, phosphofructokinase and phosphoenolpyruvate carboxykinase in white muscle and red muscle, Biochem. J. 103 (1967) 391–399, https://doi.org/10.1042/bj1030391.
[53] M.M. Bradford, A rapid and sensitive method for the quantitation of microgram quantities of protein utilizing the principle of protein-dye binding, Anal. Biochem. 72 (1976) 248–254, https://doi.org/10.1016/0003-2697(76)90527-3.
[54] Y. Meng, L. Zong, Estrogen stimulates SREBP2 expression in hepatic cell lines via an estrogen response element in the SREBP2 promoter, Cell. Mol. Biol. Lett. 24 (2019) 65, https://doi.org/10.1186/s11658-019-0194-5.
[55] S.-J. Cho, M. Ning, Y. Zhang, L.H. Rubin, H. Jeong, 17β-Estradiol up-regulates UDP-glucuronosyltransferase 1A9 expression via estrogen receptor α, Acta Pharm. Sin. B. 6 (2016) 504–509, https://doi.org/10.1016/j.apsb.2016.04.005.
[56] M.K. Nagamine, T.C. da Silva, P. Matsuzaki, K.C. Pinello, B. Cogliati, C.R. Pizzo, G. Akisue, M. Haraguchi, S.L. Górniak, I.L. Sinhorini, K.V.K. Rao, J.A.M. Barbuto, M.L.Z. Dagli, Cytotoxic effects of butanolic extract from Pfaffia paniculata (Brazilian ginseng) on cultured human breast cancer cell line MCF-7, Exp. Toxicol. Pathol. 61 (2009) 75–82, https://doi.org/10.1016/j.etp.2008.01.017.
[57] Y.Y. Li, H.S. Wu, L. Tang, C.R. Feng, J.H. Yu, Y. Li, Y.S. Yang, B. Yang, Q.J. He, The potential insulin sensitizing and glucose lowering effects of a novel indole derivative in vitro and in vivo, Pharmacol. Res. 56 (2007) 335–343, https://doi.org/10.1016/j.phrs.2007.08.002.
[58] R.C. Scaduto, L.W. Grotyohann, Measurement of mitochondrial membrane potential using fluorescent rhodamine derivatives, Biophys. J. 76 (1999) 469–477, https://doi.org/10.1016/S0006-3495(99)77214-0.
[59] H. Wang, J.A. Joseph, Quantifying cellular oxidative stress by dichlorofluorescein assay using microplate reader, Free Radic. Biol. Med. 27 (1999) 612–616, https://doi.org/10.1016/S0891-5849(99)00107-0.